Extending the Solvent Acidiy Scale to Highly Acidic Organic Solvents: The Unique Photophysical Behaviour of 3,6-Diethyltetrazine

Javier Catalán*[a] and Cristina Díaz[a]

Keywords: Solvent acidity scale / Solvent effects / Solvatochromism

The SA scale, developed previously for weakly acidic solvents, was extended to include the most acidic solvents (haloalcohols and carboxylic acids) by using a unique solvatochromic probe (3,6-diethyl-1,2,4,5-tetrazine). The proposed new solvent scale has a number of advantages over widely used alternatives such as that based on Gutmann's acceptor number (AN). As shown in this paper, SA data provide an accurate description of the effect of solvent acidity on various chemical properties.

The solvent in which a physical process takes place is often a non-inert medium that plays a major role in solution chemistry. Roughly, the solvent effect can be resolved into non-specific, and specific solute−solvent interactions.[1] In previous papers, we reported scales accurately describing solvent effects such as the Solvent Polarity/Polarizability (SPP) scale[2] for non-specific contributions, and the Solvent Acidity (SA)[3] and Solvent Basicity (SB)[4] scales for specific contributions.

The SPP scale is based on the solvatochromism of the probe 2-(dimethylamino)-7-nitrofluorene (DMANF) and its homomorph 2-fluoro-7-nitrofluorene (FNF) and encompasses values between 1 for dimethyl sulfoxide and 0 for the gas phase. The SB scale is based on the solvatochromism of the probe 5-nitroindoline (NI) and its homomorph 1-methyl-5-nitroindoline (MNI) and encompasses values between 1 for tetramethylguanidine and 0 for the gas phase. Both scales are currently extended to about 200 solvents.

While the SPP and SB scales encompass solvents of high and low polarity and basicity, the SA scale could initially not be extended to solvents of low and moderate acidity, in which the stilbene betaines used are soluble and remain in neutral form. Specifically, the SA scale was originally based on the solvatochromism of the *o-tert*-butylstilbazolium betaine (TBSB)/*o,o'*-di-*tert*-butylstilbazolium betaine (DTBSB) probe/homomorph pair; however, the high basicity of these probes − pK_a for DTBSB is about 10[5] − makes them useless for examining solvents more acidic than methanol (SA = 0.605). Also, residual moisture or acid traces in the solvents can protonate the probes and render them unusable. These shortcomings led us to search for a less acidic but sensitive enough probe to measure the acidity of solvents such as carboxylic acids and haloalcohols.

A suitable acidity probe for acid solvents should be basic enough to not result in its protonation by such solvents; however, it should also be sensitive enough to acidity to allow its precise determination. Ever since Kasha introduced and characterized it in his pioneering work,[6][7] the $n \rightarrow \pi^*$ electron transition has been known to be of weak intensity and to undergo a hypsochromic shift in the presence of acidic solvents, whereas protonation causes the $n \rightarrow \pi^*$ transition to vanish. There have been many attempts at using this transition to characterize solvents;[8] however, its low intensity and its tendency to be masked by $\pi \rightarrow \pi^*$ transitions in the presence of acidic and basic solvents − which displace it to higher energy levels − detract from its potential.

A probe exhibiting an $n \rightarrow \pi^*$ transition will only be suitable for measuring the acidity of highly acidic solvents if (i) it is not so basic that it will undergo ready protonation; (ii) its dipole moment is small enough for the $n \rightarrow \pi^*$ transition to be insensitive to the solvent polarity; and (iii) its first $\pi \rightarrow \pi^*$ transition is bathochromically shifted to an adequate extent so that it will not overlap with the $n \rightarrow \pi^*$ transition when estimating solvent acidities; this can be accomplished by displacing the *n* molecular orbital to a lower energy level, either by short-range electrostatic effects such as lone pair repulsions[9] or by antibonding features in the molecular orbitals containing the lone pairs of the chromophor.[10] All these features meet in 1,2,4,5-tetrazine (*s*-tetrazine), a unique chromophore with pK_a < 0,[11] a near-zero overall dipole moment and an $S_0 \rightarrow S_1$ transition of the $n \rightarrow \pi^*$ type with a maximum in cyclohexane at λ_{max} = 542 nm[11] that is quite distant from its first $\pi \rightarrow \pi^*$ transition, which occurs at λ_{max} = 252 nm;[11] however, its rapid photochemical decomposition[12] into one nitrogen molecule and two hydrogen cyanide molecules (Scheme 1) render it unusable.

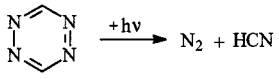

Scheme 1. Photochemical decomposition of *s*-tetrazine

In this work, we examined 3,6-diethyl-1,2,4,5-tetrazine (DETZ), which, in addition to possessing the interesting photophysical properties of *s*-tetrazine, is photostable. By using this probe, we extended the SA scale to carboxylic acids, phenols, haloalcohols, and halocarboxylic acids such as trifluoroacetic acid. The SPP and SB values for the new solvents included in the scale are reported and additional

[a] Departamento de Química Física Aplicada, Universidad Autónoma de Madrid,
Cantoblanco, E-28049 Madrid, Spain

  1434−193X/99/0404−0885 $ 17.50+.50/0

information for such a significant solvent as water is provided.

Results and Discussion

Tables 1−4 collate the results obtained, which are discussed below.

s-Tetrazine possesses two lone electron pairs located on opposite sites of its hexagonal ring; the strong interaction between the two pairs results in one antibonding *n* orbital in the compound lying at an anomalously high energy; this, as shown below, has special spectroscopic implications. The

Table 1. Wavenumbers for the maximum of the first absorption band for the probe 2-(dimethylamino)-7-nitrofluorene ($\tilde{\nu}_{DMANF}$) and its homomorph 2-fluoro-7-nitrofluorene ($\tilde{\nu}_{FNF}$); differences of $\tilde{\nu}_{DMANF}$ and $\tilde{\nu}_{FNF}$ ($\Delta\tilde{\nu}$, cm^{-1}) and their normalized SPP values

n	Solvent	$\tilde{\nu}_{DMANF}$	$\tilde{\nu}_{FNF}$	$\Delta\tilde{\nu}$	SPP
1	trimethylacetic acid	24752	30780	6028	0.630
2	isobutyric acid	24519	30573	6054	0.643
3	isovaleric acid	24452	30515	6063	0.647
4	nonanoic acid	24411	30488	6077	0.653
5	valeric acid	24421	30503	6082	0.656
6	hexanoic acid	24420	30503	6083	0.656
7	butyric acid	24387	30481	6094	0.662
8	heptanoic acid	24402	30497	6095	0.662
9	octanoic acid	24416	30513	6097	0.663
10	propionic acid	24281	30435	6154	0.690
11	2-methylbutyric acid	24449	30614	6165	0.695
12	1,2-butanediol	23388	29985	6597	0.899
13	2,3-butanediol	23320	29927	6607	0.904
14	formic acid	22880[a]	29498	6618	0.909
15	2,2,3,3-tetrafluoro-1-propanol	22821[a]	29448	6627	0.913
16	2-methyl-1,3-propanediol	23161	29812	6651	0.924
17	1,2-propanediol	23220	29875	6655	0.926
18	2,2,3,4,4,4-hexafluoro-1-butanol	22507[a]	29182	6675	0.936
19	1,3-butanediol	23207	29899	6692	0.944
20	1,4-butanediol	23104	29809	6705	0.950
21	1,3-propanediol	23056	29763	6707	0.951
22	dichloroacetic acid	21961[a]	28720	6759	0.975
23	pentafluoropropionic acid	21542[a]	28365	6823	1.006
24	trifluoroacetic acid	21407[a]	28251	6844	1.016
25	α,α,α-trifluoro-*m*-cresol	20436[a]	27428	6992	1.085

[a] Calculated from $\tilde{\nu}_{DMANF} = (1.181 \pm 0.026)\ \tilde{\nu}_{FNF} - 11957$.[13]

Table 2. Wavenumbers for the maximum of the first UV/Vis absorption band for the probe 5-nitroindoline ($\tilde{\nu}_{NI}$) and its homomorph 1-methyl-5-nitroindoline ($\tilde{\nu}_{MNI}$); differences of $\tilde{\nu}_{NI}$ and $\tilde{\nu}_{MNI}$ ($\Delta\tilde{\nu}$, cm^{-1}) and their normalized SB values

n	Solvent	$\tilde{\nu}_{NI}$	$\tilde{\nu}_{MNI}$	$\Delta\tilde{\nu}$	SB
1	water	23725	22199	1526	0.025
2	trimethylacetic acid	27522	26178	1344	0.130
3	2-methylbutyric acid	26894	25758	1136	0.250
4	isobutyric acid	26775	25693	1082	0.281
5	heptanoic acid	26756	25756	1000	0.328
6	propionic acid	26319	25403	916	0.377
7	isovaleric acid	26524	25657	867	0.405
8	1,3-propanediol	24347	23669	678	0.514
9	1,2-propanediol	24493	23960	533	0.598
10	1,4-butanediol	24444	23912	532	0.598
11	1,3-butanediol	24459	23948	511	0.610
12	2-methyl-1,3-propanediol	24412	23910	502	0.615
13	2,3-butanediol	24465	24027	438	0.652
14	1,2-butanediol	24608	24198	410	0.668

Table 3. Wavenumbers for the UV/Vis maximum of the first absorption band for the probe *o*-*tert*-butylstilbazolium betaine dye ($\tilde{\nu}_{TBSB}$) and its homomorph *o*,*o*′-di-*tert*-butylstilbazolium betaine dye ($\tilde{\nu}_{DTBSB}$) and their normalized SA values

n	Solvent	$\tilde{\nu}_{DTBSB}$	$\tilde{\nu}_{TBSB}$	$\Delta\tilde{\nu}$	SA
1	1,3-butanediol	16329	18045	1393.1	0.429
2	1,4-butanediol	16406	18139	1378.9	0.424
3	1,2-butanediol	16421	18295	1513.8	0.466

Table 4. Wavenumbers for the maximum of the $n \rightarrow \pi^*$ transition in the DETZ probe and corresponding SA values

Solvent	SPP	$\tilde{\nu}_{DETZ}$	$\Delta\tilde{\nu}$(kK)	SA
methylpiperidine	0.622	18132		
methylpyrrolidine	0.631	18191		
N-methylcyclohexylamine	0.664	18178		
N,*N*-dimethylcyclohexylamine	0.667	18145		
2-methyltetrahydrofuran	0.717	18258		
butylamine	0.730	18252		
isoamyl acetate	0.752	18271		
ethyl acetate	0.795	18336		
tetrahydrofuran	0.838	18332		
2-butanone	0.881	18402		
butyronitrile	0.915	18453		
N,*N*-diethylacetamide	0.930	18475		
1,1,3,3-tetramethylurea	0.952	18457		
nonanoic acid	0.653	18267	0.093	0.416
1,3-butanediol	0.944	18566	0.097	0.429[a]
1,4-butanediol	0.950	18575	0.100	0.424[a]
octanoic acid	0.663	18284	0.100	0.422
2-methylbutyric acid	0.695	18336	0.120	0.439
1,2-butanediol	0.899	18549	0.126	0.466[a]
N-methylformamide	0.920	18571	0.126	0.444
chloroacetonitrile	0.896	18547	0.127	0.445
heptanoic acid	0.662	18310	0.127	0.445
2-methyl-1,3-propanediol	0.924	18584	0.135	0.451
2,3-butanediol	0.904	18575	0.147	0.461
hexanoic acid	0.656	18329	0.152	0.465
ethanol	0.853	18532	0.155	0.400[b]
trimethylacetic acid	0.630	18309	0.159	0.471
1,2-propanediol	0.926	18615	0.164	0.475
1,3-propanediol	0.951	18653	0.177	0.486
valeric acid	0.656	18373	0.196	0.502
isobutyric acid	0.643	18376	0.212	0.515
isovaleric acid	0.647	18407	0.239	0.538
2-chloroethanol	0.893	18686	0.269	0.563
methanol	0.857	18651	0.270	0.605[b]
ethylene glycol	0.932	18728	0.271	0.565
butyric acid	0.662	18462	0.279	0.571
2,2,2-trichloroethanol	0.960	18784	0.299	0.588
pyrrole	0.838	18673	0.312	0.599
propionic acid	0.690	18534	0.323	0.608
propargyl alcohol	0.915	18765	0.326	0.610
glycerol	0.948	18808	0.335	0.618
formamide	0.833	18758	0.402	0.674
acetic acid	0.781	18724	0.420	0.689
m-cresol	1.000	18956	0.430	0.697
α,α,α-trifluoro-*m*-cresol	1.085	19121	0.509	0.763
2,2,3,4,4,4-hexafluoro-1-propanol	0.936	19092	0.631	0.864
2,2,3,3-tetrafluoro-1-propanol	0.913	19072	0.634	0.867
2,2,2-trifluoroethanol	0.908	19098	0.665	0.893
1,1,1,3,3,3-hexafluoro-2-propanol	1.007	19340	0.807	1.011
formic acid	0.909	19245	0.812	1.015
dichloroacetic acid	0.975	19321	0.821	1.023
water	0.962	19355	0.868	1.062
trifluoroacetic acid	1.016	19704	1.162	1.307
pentafluoropropionic acid	1.006	19718	1.186	1.327

[a] See Table 3. − [b] Ref.[3]

π-electron system of *s*-tetrazine is similar to that of benzene. Thus, the first $\pi \rightarrow \pi^*$ transition in the two systems appears at $\lambda_{max} = 252$ for *s*-tetrazine and 260 nm for benzene. On the other hand, the $n \rightarrow \pi^*$ transition in *s*-tetrazine is strongly shifted to the visible region ($\lambda_{max} \approx 550$ nm), which is the origin of its deep colour. This unique feature makes this compound a firm candidate for use as an environmental probe as the wide energy gap between the two transitions excludes a potential overlap.

The spectra for DETZ in cyclohexane and water (Figure 1) confirm the wide energy gap between the first $n \rightarrow \pi^*$ electron transition, which peaks at $\lambda_{max} = 550$ nm, and the first $\pi \rightarrow \pi^*$ transition of the chromophore, with its maximum at $\lambda_{max} = 270$ nm; however sensitive these transitions may be to the nature of a given solvent, overlap between the two transitions can reliably be discarded. Tests involving sulphuric acid have revealed that, like *s*-tetrazine,[11] DETZ must have a pK_a below zero, so a potential protonation of the probe by a solvent can also be ruled out. Obviously, DETZ has a small dipole moment ($\mu = 0.38$ Debye as derived from B3LYP/6-31G** computations); as a result, any hypsochromic shift in its $n \rightarrow \pi^*$ transition by effect of an increased solvent polarity will be small. The beautiful fuchsia colour of the probe in the solvents studied is not lost upon irradiation during solvent acidity measurements − even after several hours. Nor is its UV/Vis spectrum appreciably altered. Consequently, DETZ appears to be photostable enough for use as an environmental probe.

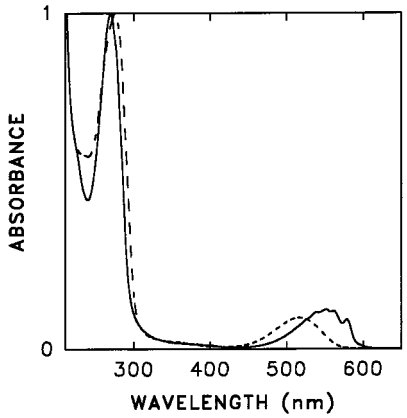

Figure 1. UV/Vis spectra of DETZ normalized at the maximum in cyclohexane (—) and water (- - -)

The sensitivity of the $n \rightarrow \pi^*$ transition in DETZ to the solvent is clearly reflected in its UV/Vis spectra in methylcyclohexane, methanol, trifluoroethanol, hexafluoro-2-propanol, acetic acid, and trifluoroacetic acid (Figure 2), with maxima at $\lambda = 550$, 536, 524, 517, 534, and 507 nm, respectively. In addition, the spectral envelope undergoes no significant change in the solvents studied, so a potential protonation of the probe − even a partial one − can be discarded.

The shift in the $n \rightarrow \pi^*$ band is largely caused by the solvent acidity; however, an $n \rightarrow \pi^*$ transition is also obviously sensitive to the medium polarity, the contribution of which must thus be subtracted if the medium acidity is to

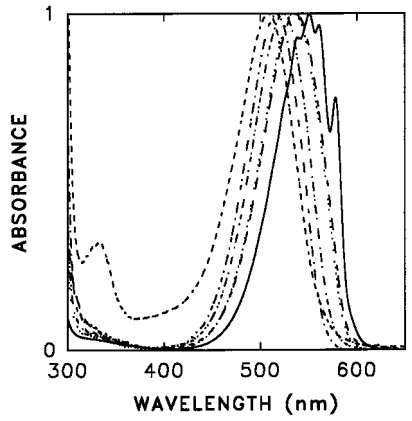

Figure 2. UV/Vis spectra of DETZ normalized at the maximum in methylcyclohexane (—), methanol (− − −), 2,2,2,-trifluoroethanol (−·· −·· −), 1,1,1,3,3,3-hexafluoro-2-propanol (−·−·−), acetic acid (···) and trifluoroacetic acid (— — —)

be accurately determined. To this end, we used the solvatochromic method of Taft and Kamlet[14] to plot the frequency of the absorption maximum for the $n \rightarrow \pi^*$ transition against the solvent polarity (its SPP value). As can be seen from Figure 3, non-acidic solvents exhibit a linear behaviour (Equation 1), whereas acidic solvents depart from it to an extent proportional to their acidity.

$$\tilde{\nu}_{DETZ} = (1.0147 \pm 0.0579)\ SPP + (17.511 \pm 0.045) \quad (1)$$

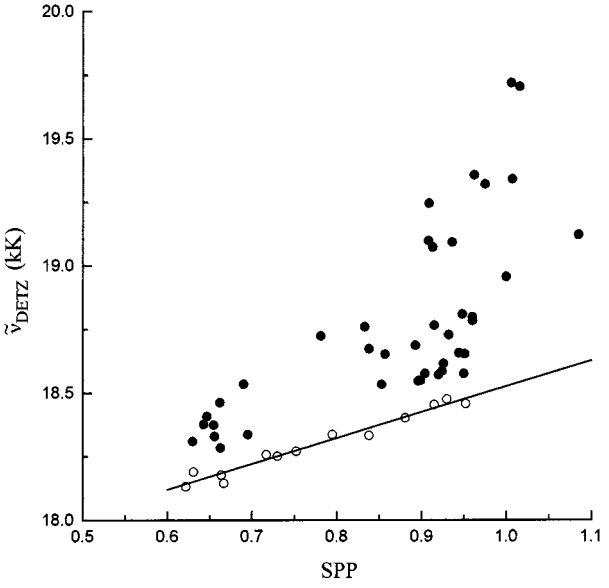

Figure 3. Plot of wavenumber for the maximum of the $n \rightarrow \pi^*$ transition of DETZ against SPP polarity

($n = 13$, $r = 0.983$, $sd = 23\ cm^{-1}$)

Table 4 gives the shifts, $\Delta\nu_{DETZ}$, of the acidic solvents from this straight line. In order to translate these data to our SA scale, we used solvents with SA > 0.4 (viz. 1,2-butanediol, 1,3-butanediol, ethanol, methanol, and hexafluoro-2-propanol) and adopted SA = 1.00 for such an acidic solvent as hexafluoro-2-propanol. The relation given in Equation 2 between the two scales was obtained.

$$SA = (0.833 \pm 0.068)\,\Delta\tilde{\nu}_{DETZ} + (0.339 \pm 0.024) \quad (2)$$
$$(n = 6,\ r = 0.987,\ sd = 0.041\ kK)$$

Equation 2 was used to determine the SA values for the acidic solvents; this obviously resulted in decreased precision with the less acidic solvents (viz. those with $\Delta\tilde{\nu}_{DETZ} < 100\ cm^{-1}$). In any case, Equation 2 can be used to estimate SA for moderately acidic solvents (viz. those with $\Delta\tilde{\nu}_{DETZ}$ values in the range of $\Delta\tilde{\nu} = 50-100\ cm^{-1}$) not directly measurable with the TBSB/DTBSB pair.

Table 4 gives the SA values for the solvents studied. SA for carboxylic acids decreases with increasing chain length (see Figure 4); the variation is similar to that of the acidity of alkanols when measured with the TBSB/DTBSB pair (Figure 5). It is worth noting the high acidity of water (SA = 1.062), a likely result of self-clustering, which also decreases its basicity to a drastic extent (SB = 0.025).

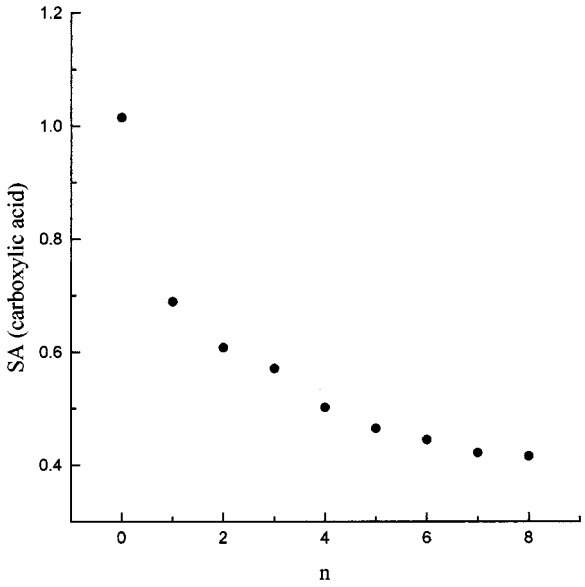

Figure 4. Plot of SA against the number of carbon atoms in the carboxylic acids studied

Correlation of Experimental Data with the SA Scale

The applicability of our scale to data obtained by using other spectroscopic techniques and alternative chemical means is examined below. The cases discussed and data reported were both from the same laboratory whenever possible. Evidence was obtained from the bulk solvent in every case and only in very specific cases was the variation of solvent acidity found to be the only source of the phenomenon.

IR Data

The S=O stretching frequencies of dimethyl sulfoxide (DMSO), dissolved in pure solvents, were recently studied by Fawcett and Kloss[15] in probing the solvent effect; they found such frequencies to be strongly correlated with Gutmann's acceptor number (AN).[16] This conclusion was relatively predictable since AN values were derived from the behaviour of Et_3PO towards the solvent and the solvent-active site in both DMSO and Et_3PO appears to be the X=O group. Strangely, compounds at the top of the polarity scale (e.g. DMSO and Et_3PO, with SPP values of 1.0 and 0.908, respectively) are not affected by the solvent polarity; in fact, the S=O stretching frequencies for DMSO determined by Fawcett are accurately reproduced by the SA and SPP values for the solvents by the relation given in Equation 3.

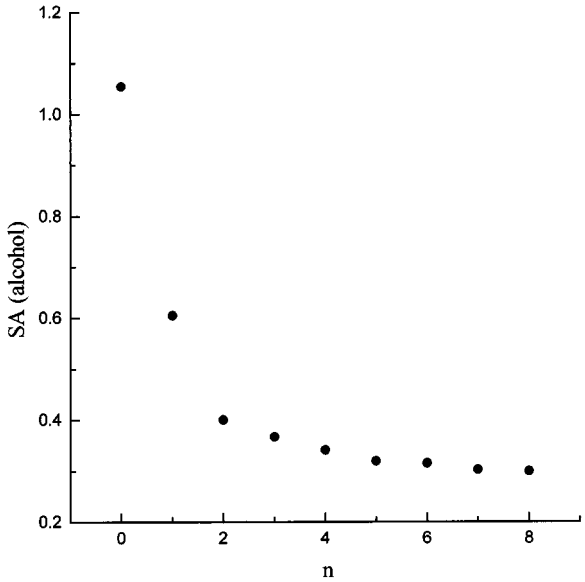

Figure 5. Plot of SA against the number of carbon atoms in the alcanols studied

$$\tilde{\nu}^{S=O}\,(DMSO) = -89.67\ (\pm 4.60)\ SA - 38.90\ (\pm 7.50)\ SPP + 1099.10\ (\pm 6.5) \quad (3)$$
$$(n = 21,\ r = 0.979,\ sd = 6.8\ cm^{-1})$$

As can be seen from Figure 6, consistency is reasonable taking into account that the correlation encompasses media ranging from trifluoroacetic acid to the gas phase.

UV/Vis Absorption Data

As can be seen from Figure 7, the absorption maxima for *N*-methylacridone (MA) determined by Siegmund and Bendig[17] are also reproduced by our polarity and acidity parameters by the relation given in Equation 4.

$$\tilde{\nu}_{abs}\,(MA) = -0.62\ (\pm 0.06)\ SA - 1.59\ (\pm 0.12)\ SPP + 26.48\ (\pm 0.09) \quad (4)$$
$$(n = 29,\ r = 0.970,\ sd = 0.08\ kK)$$

In 1985, Wrona et al.[8c] developed a Lewis acidity scale (the $E_B{}^N$ scale) from measurements of the absorption maxima for the $n \rightarrow \pi^*$ transition in the 2,2,6,6-tetramethylpiperidine *N*-oxyl (TMPNO) radical. Parameter $E_B{}^N$ is de-

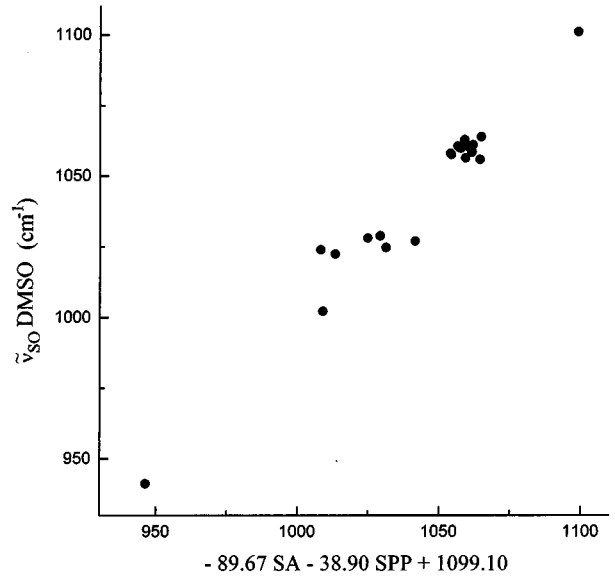

Figure 6. S=O stretching frequencies for DMSO in various solvents as a function of the corresponding SA and SPP values

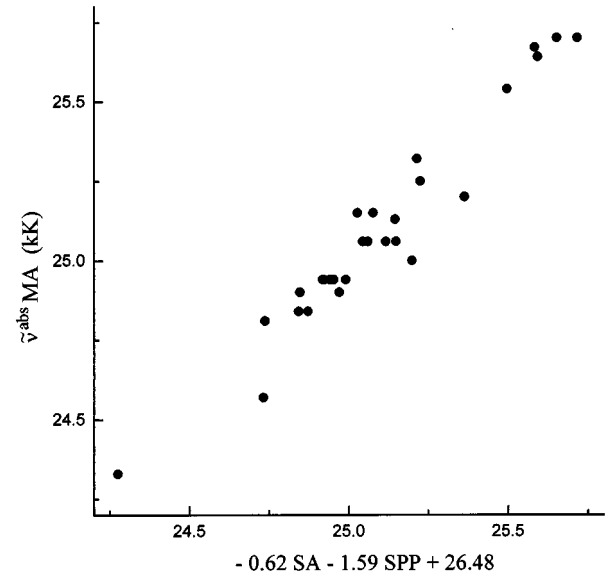

Figure 7. Wavenumbers for the UV/Vis absorption maximum of *N*-methylacridone in various solvents as a function of the SA and SPP values for the solvents

fined as the energy, in kJ mol^{-1}, of the $n \rightarrow \pi^*$ transition in the TMPNO spectrum as recorded in various solvents.

Based on the SA scale (Figure 8), HBD solvents are correlated with the absorption maxima for the $n \rightarrow \pi^*$ band of TMPNO in 37 solvents by Equation 5.

$$\tilde{\nu}_{abs}(\text{TMPNO}) = 1.95\ (\pm 0.09)\ \text{SA} + 21.45\ (\pm 0.03) \quad (5)$$
$$(n = 37,\ r = 0.963,\ sd = 0.13\ \text{kK})$$

Kinetic Data

The proton transfer in 7-azaindole (7AI)/alcohol systems in the excited state is a two-step process[18] (see Scheme 2).

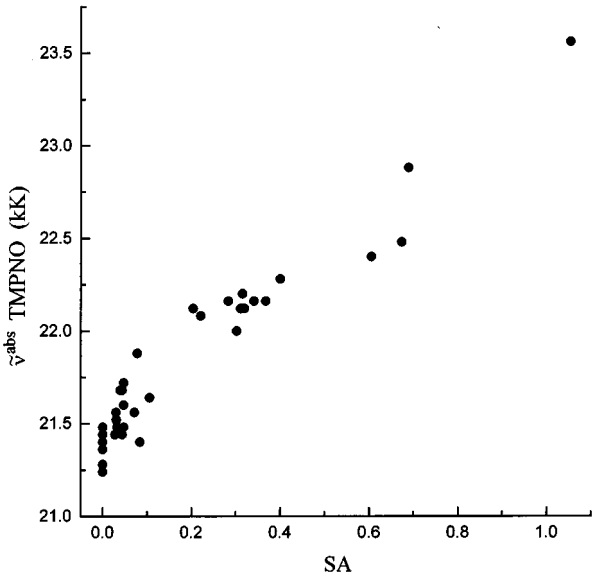

Figure 8. Wavenumbers for the maximum of the $n \rightarrow \pi^*$ absorption band of TMPNO in various solvents as a function of the corresponding SA values

The first step involves a dynamic rearrangement of the solvent around the excited 7AI molecule to a configuration enabling tautomerization. The second is a rapid, irreversible step involving a dual proton transfer to yield the tautomeric species.

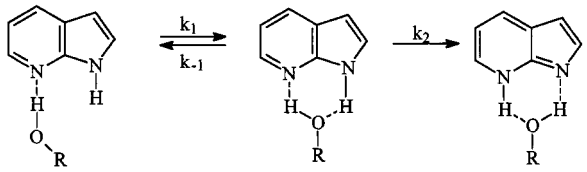

Scheme 2. Proton transfer in 7-azaindole/alcohol system

The rate of this reaction varies with the particular alcohol (specifically, with the strength of the hydrogen bond between 7AI and the solvent); it is thus related to the ability of the alcohol to release its hydroxy proton.

Figure 9 shows a plot of the proton-transfer lifetimes calculated by Maroncelli et al.[18] against the SA values for 12 alcohols; as can be seen, the two variables are well correlated (the rate of proton transfer decreases with increasing acidity of the alcohol) by Equation 6.

$$\tau_{ps}\ (7\text{AI}) = -315.97\ (\pm 14.47)\ \text{SA} + 319.47\ (\pm 7.43) \quad (6)$$
$$(n = 12,\ r = 0.990,\ sd = 12.75\ \text{ps})$$

Thermodynamic Data

Abraham et al.[19] calculated the solvent effects on the Gibbs energy for the transition state of *tert*-butyl chloride solvolysis and found it to be virtually exclusively affected by the polarity and acidity of the hydrogen bond.

Figure 10 shows a plot of $\delta\Delta G^{\neq}$ (obtained as the difference between $\Delta G^{\neq}$ in each solvent and the $\Delta G^{\neq}$ value for *N*,*N*-dimethylformamide as reference) against SA and SPP.

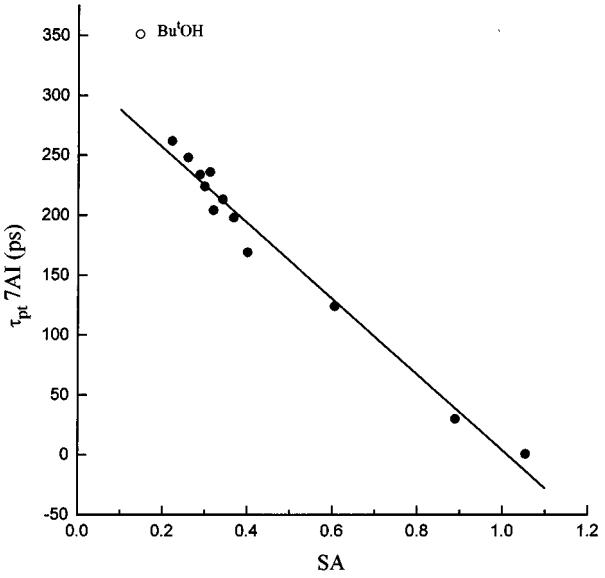

Figure 9. Lifetimes for the proton transfer from 7-azaindole to various alcohols as a function of SA for the alcohols

While non-HBD solvents deviate from the linear behaviour of HBD solvents in Figure 10a, both types of solvent exhibit a linear trend with SA and SPP (Equation 7) in Figure 10b, consistent with the findings of Abraham et al.[19]

$$\delta\Delta G^{\neq}\ (t\text{BuCl}) = -9.85\ (\pm 0.55)\ \text{SA} - 11.45\ (\pm 2.16)\ \text{SPP} + 12.13\ (\pm 1.87) \quad (7)$$
$$(n = 30,\ r = 0.966,\ sd = 1.00\ \text{kcal.mol}^{-1})$$

Comparison of the SA Scale with Other Solvent Acidity Scales

AN Scale

The AN scale, developed in 1975 by Gutmann et al.[16] to characterize the electrophilic properties of solvents, is based on measurements of the NMR chemical shifts of the ^{31}P nucleus of triethylphosphane oxide, extrapolated to infinite dilution, with diphenylphosphinic acid as external standard. As can be seen from Figure 11, the two scales are related, with the sole exception of trifluoroacetic acid. This deviation can be explained as follows: In this solvent, an amount of protonated trimethylphosphane oxide comparable to that of the adduct formed between the oxide and the acid is present, so the ^{31}P signal represents the average of the two situations.

$$\text{AN} = 41.75\ (\pm 2.92)\ \text{SA} + 15.81\ (\pm 1.11) \quad (8)$$
$$(n = 20,\ r = 0.958,\ sd = 3.85)$$

$E_T(30)$ Scale

The $E_T(30)$ scale of Dimroth and Reichardt,[20] based on the negative solvatochromism of 2,6-diphenyl-4-(2,4,6-triphenyl-1-pyridinio)phenoxide and defined by the position

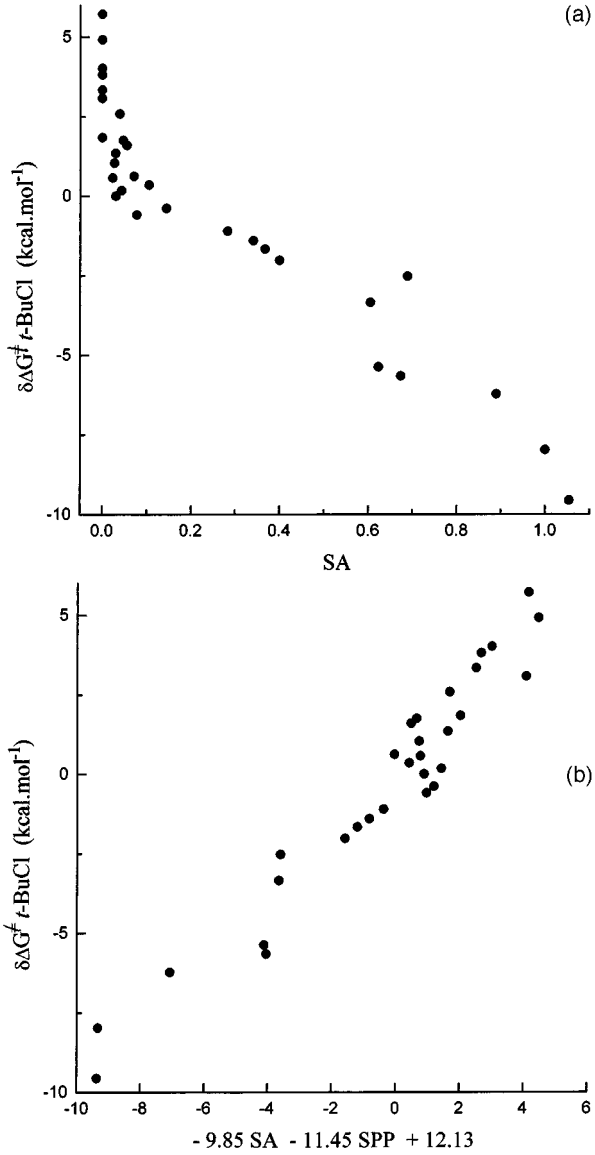

Figure 10. Variation of the Gibbs energy of activation of *tert*-butyl chloride solvolysis in various solvents as a function of (a) SA and (b) SA and SPP at 298 K

(in kcal·mol^{-1}) of the maximum of the first absorption band for this dye, was initially conceived as a polarity scale. However, this betaine was later found to also exhibit specific hydrogen-bonding interactions, which was used by Koppel and Palm[21] to develop their *E* Lewis acidity scale (electrophilic solvating power) from the $E_T(30)$ scale as corrected for the influence of non-specific effects.

Figure 12 shows the E_T^N values for 88 different solvents against the corresponding SA and SPP values. As can be seen, the two sets of values are quite well correlated by Equation 9.

$$E_T^N = 0.74\ (\pm 0.02)\ \text{SA} + 0.50\ (\pm 0.10)\ \text{SPP} - 0.12\ (\pm 0.09) \quad (9)$$
$$(n = 88,\ r = 0.958,\ sd = 0.06)$$

Experimental Section

All solvents used were of the highest available purity and purchased from Aldrich or Fluka. 3,6-Diethyl-1,2,4,5-tetrazine (DETZ) was

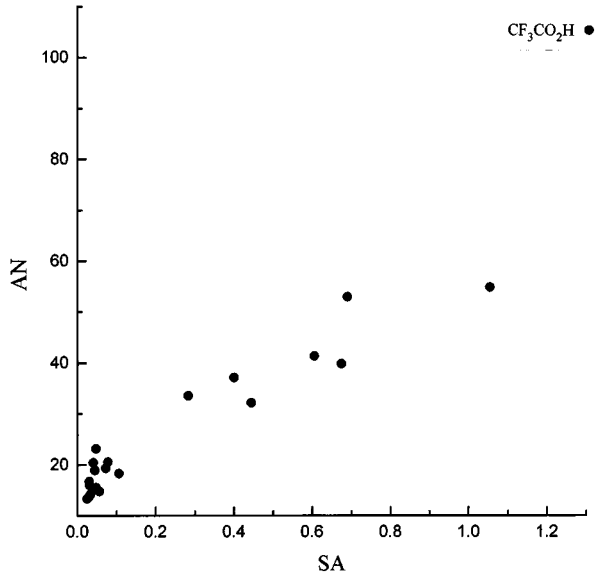

Figure 11. Plot of AN against SA for various solvents

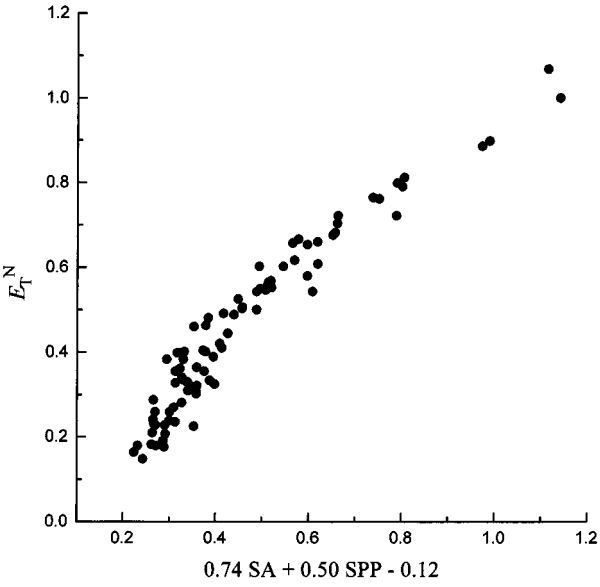

Figure 12. Plot of E_T^N against SA and SPP for various solvents

obtained according to a procedure described elsewhere.[22] UV/Vis measurements were made with a Shimadzu 2100 spectrophotometer the monochromator of which was calibrated for the 486.0- and 656.1-nm lines from a deuterium lamp. The instrument was routinely checked for wavelength accuracy by using holmium–didymium filters. All spectral measurements were made at 25°C, using a pair of matched quartz cells of 1 cm path length. The maximum-absorption wavelength was determined from the derivative function. The results given are the arithmetic means of at least 8 spectra whose maxima were shifted by less than 0.2 nm.

Acknowledgments

We are greatly indebted to DGICYT of Spain (Project No. PB93-0280) for financial support. C. D. thanks the Comunidad Autónoma de Madrid for a postdoctoral grant.

[1] C. Reichardt, *Solvents and Solvent Effects in Organic Chemistry*, 2nd ed., VCH Publishers, Weinheim, **1988**, and references therein.
[2] J. Catalán, V. López, P. Pérez, R. Martín-Villamil, J.-G. Rodríguez, *Liebigs Ann.* **1995**, 241–252.
[3] J. Catalán, C. Díaz, *Liebigs Ann.* **1997**, 1941–1949.
[4] J. Catalán, C. Díaz, V. López, P. Pérez, J.-L. G. de Paz, J.-G. Rodríguez, *Liebigs Ann.* **1996**, 1785–1794.
[5] I. Gruda, F. Bolduc, *J. Org. Chem.* **1984**, *49*, 3300–3305.
[6] M. Kasha, *Discuss. Faraday Soc.* **1950**, N9, 14–19.
[7] G. J. Breadley, M. Kasha, *J. Am. Chem. Soc.* **1955**, *77*, 4462–4468.
[8] [8a] J. E. Dubois, A. Bienvenüe, *J. Chim. Phys.* **1968**, *65*, 1259–1265. – [8b] W. Walter, O. H. Bauer, *Justus Liebigs Ann. Chem.* **1977**, 421–429. – [8c] A. Janowski, I. Turowska-Tyrk, P. K. Wrona, *J. Chem. Soc., Perkin Trans. 2* **1985**, 821-825.
[9] [9a] R.W. Taft, F. Anvia, M. Taagepera, J. Catalán, J. Elguero, *J. Am. Chem. Soc.* **1986**, *108*, 3237–3239. – [9b] J. Catalán, J. Palomar, J.-L. G. de Paz, *Int. J. Mass Spectrom. Ion Processes* **1998**, *175*, 51–59.
[10] [10a] R. Hoffmann, A. Imamura, W. J. Hehre, *J. Am. Chem. Soc.* **1968**, *90*, 1499–1509. – [10b] R. Hoffmann, *Acc. Chem. Res.* **1971**, *4*, 1–9.
[11] S. F. Mason, *J. Chem. Soc.* **1959**, 1240–1262.
[12] D. S. King, C. T. Denny, R. M. Hochstrasser, A. B. Smith III, *J. Am. Chem. Soc.* **1977**, *99*, 271–273.
[13] J. Catalán, V. López, P. Pérez, *Liebigs Ann.* **1995**, 793–795.
[14] M. J. Kamlet, R. W. Taft, *J. Am. Chem. Soc.* **1976**, *98*, 377–383 and 2886–2894.
[15] W. R. Fawcett, A. A. Kloss, *J. Phys. Chem.* **1996**, *100*, 2019–2024.
[16] U. Mayer, V. Gutmann, W. Gerger, *Monatsh. Chem.* **1975**, *106*, 1235–1257.
[17] M. Siegmund, J. Bendig, *Z. Naturforsch., A* **1980**, *35a*, 1076–1086.
[18] R. S. Moog, M. Maroncelli, *J. Phys. Chem.* **1991**, *95*, 10359–10369.
[19] M. H. Abraham, P. L. Grellier, A. Nasehzadeh, R. A. C. Walker *J. Chem. Soc., Perkin Trans 2* **1988**, 1717–1724.
[20] [20a] K. Dimroth, C. Reichardt, T. Siepmann, F. Bohlmann, *Justus Liebigs Ann. Chem.* **1963**, *661*, 1–37. – [20b] K. Dimroth, C. Reichardt, *Justus Liebigs Ann. Chem.* **1969**, *727*, 93–105. – [20c] C. Reichardt, *Justus Liebigs Ann. Chem.* **1971**, *752*, 64–67. – [20d] C. Reichardt, *Angew. Chem. Int. Ed. Engl.* **1979**, *18*, 98–110. – [20e] C. Reichardt, *Chem. Soc. Rev.* **1992**, *21*, 147–153. – [20f] C. Reichardt, *Chem. Rev.* **1994**, *94*, 2319–2358.
[21] I. A. Koppel, V. A. Palm in *Advances in Linear Free Energy Relationships* (Eds.: N. B. Chapman, J. Shorter), Plenum Press, London, **1972**, chapter 5, pp. 204–280.
[22] W. Skorianetz, E. Kováts, *Helv. Chim. Acta* **1970**, *53*, 251–262.

Received October 9, 1998
[O98448]